Inorg. Chem. **1992**, *31*, 563-567

Contribution from the Quantum Theory Project,
University of Florida, Gainesville, Florida 32611

Theoretical Investigation of the Electronic and Structural Properties of Pentagonal-Bipyramidal Complexes.

1. Diaqua(2,6-diacetylpyridine bis(semicarbazone))iron(II)

Shaun O. Sommerer,[†] John David Baker, M. C. Zerner,[*] and G. J. Palenik

Received July 2, 1991

The INDO model Hamiltonian, as implemented in the program ZINDO, was used to calculate optimum geometries for the seven-coordinate complex $[Fe(DAPSC)(H_2O)_2]^{2+}$ (where DAPSC = 2,6-diacetylpyridine bis(semicarbazone)), which has pentagonal-bipyramidal (PBP) geometry around the metal center. Three distinct geometries were determined corresponding to a singlet, triplet, and quintet spin state, respectively. Geometry optimization calculations showed the open-shell quintet to have the lowest overall energy of the three spin states. Bond distances and associated angles determined for the quintet spin state are in excellent agreement with those observed experimentally in the solid state for the $[Fe(DAPSC)(H_2O)(Cl)]^{2+}$ complex. Spectroscopic restricted open-shell (ROHF) and configuration-averaged Hartree–Fock (CAHF) calculations were performed on the optimized quintet geometry. An electronic spectrum is predicted for the title complex in a quintet ground spin state as is the ordering of the d-orbital energies.

Introduction

Stable pentagonal-bipyramidal, PBP, complexes of first-row transition metals are not common. Interest in this area continues to be significant due to the role of seven-coordinate species in reaction intermediates or transition states in associative reactions of six-coordinate complexes, oxidative-addition reactions of five-coordinate complexes, and dissociative reactions of eight-coordinate complexes.[1,2] Pentadentate Schiff base ligands such as 2,6-diacetylpyridine bis(semicarbazone), DAPSC, and 2,6-diacetylpyridine bis(benzoic acid hydrazone), DAPBAH, have recently been found to reproducibly form pentagonal girdles about transition-metal centers, which in turn leads to the formation of PBP complexes. By utilizing this chemistry, we have been able to isolate and structurally characterize each of the first-row transition metals (Ti–Zn) in PBP geometries.[3-11]

In this paper we report a theoretical investigation into the chemistry of these PBP complexes in which we employed semiempirical quantum mechanical methods of the intermediate neglect of differential overlap (INDO) type.[12] Our purpose was to explore the electronic and conformational characteristics of $[Fe(DAPSC)(H_2O)_2]^{2+}$ (I) (Figure 1), a PBP complex.

Calculations

In order to determine the effect of spin multiplicity on the conformation of I, separate geometry optimizations were performed on three different spin states (Figure 2). If the molecule can be assumed to be low spin (i.e. high field) and having C_{2v} symmetry, a closed-shell singlet results. An open-shell triplet can be obtained from the d-orbital splitting pattern expected from the point group D_{5h}. For a weak field, a high-spin quintet is obtained. For each multiplicity separate SCF calculations were performed.

Due to previous success in dealing with transition-metal compounds, the INDO model Hamiltonian,[12-16] as implemented in the program ZINDO, was used for all calculations. No refinement of the parameterization was found to be necessary in order to perform this study. The INDO model is appropriate for this investigation, since all one-center two-electron integrals necessary to distinguish spin states are retained.[16]

The geometry optimizations were performed using the parameters appropriate for the structure[14] and the BFGS quasi-Newton update technique[17] for each spin state and were considered converged when the norm of the gradient was less than 1.0×10^{-3} hartree/bohr. A restricted Hartree–Fock determinant was used for the closed-shell singlet. The open-shell calculations for geometry were of the restricted open-shell (ROHF) type as described elsewhere.[18] For all states the SCF was continued until successive cycles yielded differences in energy of less than 1.0×10^{-10} hartree (1 hartree = 2624.2 kJ/mol; 1 bohr = 0.5292 Å).

Discussion

Table I. Theoretical Bond Distances (Å) and Angles (deg) for Quintet $[Fe(DAPSC)(H_2O)_2]^{2+}$

Fe–O37	2.214	N2–C7	1.365
Fe–O38	2.214	C7–C8	1.398
Fe–O18	2.184	C8–C9	1.393
Fe–O19	2.184	C9–C10	1.393
Fe–N3	2.229	C10–C11	1.398
Fe–N2	2.219	C11–N2	1.366
Fe–N5	2.229	C11–C13	1.463
O18–C14	1.308	C13–C17	1.462
C14–N20	1.359	C13–N5	1.325
C14–N4	1.385	N5–N6	1.337
N4–N3	1.337	N6–C15	1.385
N3–C12	1.325	C15–N21	1.359
C12–C16	1.462	O19–N21	1.308
C12–C7	1.463		
O37–Fe–O38	170.8	N2–C7–C8	120.19
O37–Fe–O18	85.40	C7–C8–C9	119.09
O37–Fe–O19	87.72	C8–C9–C10	120.30
O37–Fe–N3	93.52	C9–C10–C11	119.05
O37–Fe–N2	94.54	C10–C11–N2	120.22
O37–Fe–N5	89.53	C11–N2–C7	121.14
O38–Fe–O18	87.39	N2–C11–C13	114.82
O38–Fe–O19	84.95	C10–C11–C13	124.96
O38–Fe–N3	89.65	C11–C13–C17	123.31
O38–Fe–N2	94.66	C17–C13–N5	123.39
O38–Fe–N5	93.46	C11–C13–N5	113.29
O18–Fe–O19	75.48	C13–N5–N6	121.18
O18–Fe–N3	71.97	N5–N6–C15	113.51
N3–Fe–N2	70.38	N6–C15–N21	118.97
N2–Fe–N5	70.40	N6–C15–O19	119.96
N5–Fe–O19	71.94	N21–C15–O19	121.03
Fe–O18–C14	115.96	C15–O19–Fe	115.91
O18–C14–N20	121.02	C20–C14–N4	119.00
O18–C14–N4	119.95	C14–N4–N3	113.62
N4–N3–C12	121.26	N3–C12–C16	123.50
C16–C12–C7	123.22	N3–C12–C7	113.26
C12–C7–N2	114.85	C12–C7–C8	124.96

The Complex $[Fe(DAPSC)(H_2O)_2]^{2+}$. Our interest in this study was to determine the effect of spin multiplicity on the conformation of this Fe–DAPSC complex, since several spin states can arise for a d^6 species such as Fe^{2+}. Specifically, we were interested in

---

[*] Corresponding author.

[†] Present address: Penn State–Erie, The Behrend College, Division of Science, Engineering and Technology, Station Road, Erie, PA 16563.

(1) Hoffmann, R.; Beier, B. F.; Muetteries, E. L.; Rossi, A. R. *Inorg. Chem.* **1977**, *16*, 511.

(2) Kepert, D. L. *Prog. Inorg. Chem.* **1979**, *25*, 41.

(3) Wester, D. W. Ph.D. Dissertation, The University of Florida, 1975.

(4) Wester, D. W.; Palenik, G. J. *J. Am. Chem. Soc.* **1973**, *95*, 6505.

(5) Wester, D. W.; Palenik, G. J. *J. Am. Chem. Soc.* **1974**, *96*, 7576.

(6) Palenik, G. J.; Wester, D. W.; Rychlewska, U.; Palenik, R. C. *Inorg. Chem.* **1976**, *15*, 1814.

(7) Palenik, G. J.; Giordano, T. *J. Chem. Soc., Dalton Trans.* **1987**, 1175.

(8) McRitchie, D. D.; Palenik, R. C.; Palenik, G. J. *Inorg. Chim. Acta* **1976**, *20*, L27.

(9) David, J.; Palenik, G. J. *Inorg. Chim. Acta* **1985**, *99*, L51.

(10) Giordano, T. J.; Palenik, G. J.; Palenik, R. C.; Sullivan, D. A. *Inorg. Chem.* **1979**, *18*, 2245.

0020-1669/92/1331-0563$03.00/0

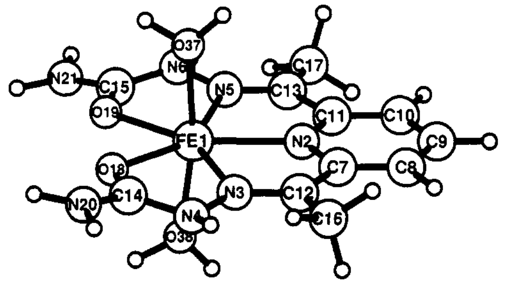

Figure 1. Illustration of the quintet-optimized geometry for the complex $[Fe(DAPSC)(H_2O)_2]^{2+}$ as determined by ZINDO.

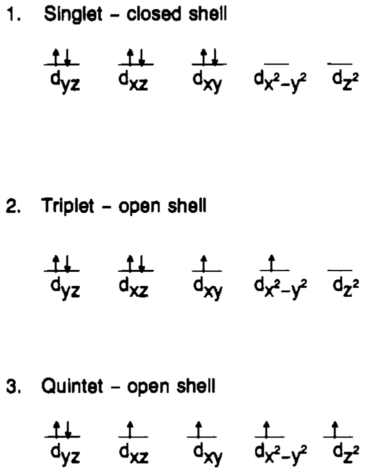

Figure 2. Illustration of the possible spin states for an Fe^{2+} (d^6) ion.

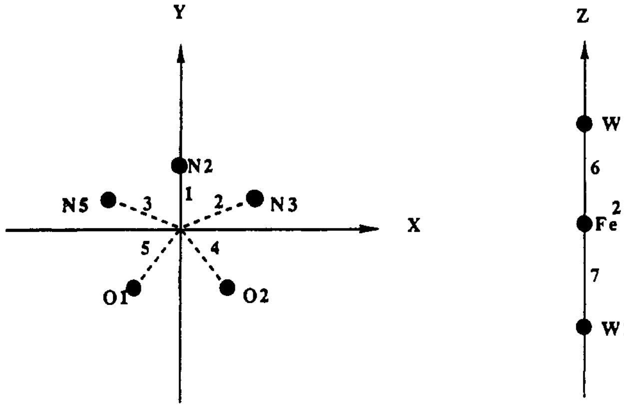

Figure 3. Coordinate system and atom-numbering scheme.

bond distances between the metal cation and the ligand donors as well as the geometry exhibited within the coordination sphere as a function of the spin state. Figure 3 displays the coordinate system used in this work as well as the atom-numbering scheme for the donors in the immediate coordination sphere, and Figure 1 illustrates the optimum geometry of the complex as determined by ZINDO for the quintet spin state. Table I is a listing of the bond distances and associated bond angles obtained from the optimization calculations for an Fe^{2+} (d^6) center in a quintet spin state. Table II summarizes the bond distances obtained from an X-ray diffraction study[4] together with those distances calculated for the optimized Fe^{2+} singlet, triplet, and quintet spin states. Table III lists the relative energy (in eV) of each possible spin state for each of the three optimized spin-state geometries. These calculated values are all relative to the optimized quintet geometry, which was found to be the lowest in total energy.

Table II. Calculated Bond Distances within the Immediate Coordination Sphere of the $Fe^{2+}(d^6)$ Complex for Several Constrained Spin States

bond[a] no.	singlet	triplet	quintet	obsd
1	2.090	2.207	2.219	2.220
2	2.165	2.226	2.229	2.229
3	2.171	2.226	2.229	2.195
4	2.238	2.177	2.184	2.192
5	2.242	2.177	2.184	2.175
6	2.160	2.152	2.214	
7	2.160	2.152	2.214	

[a] All bond distances are given in Å. Bonds are in reference to Figure 3.

Table III. Relative Energies (eV)

	structure no.		
spin multiplicity	1[a]	2[b]	3[c]
singlet	2.865	2.855	2.915
triplet	1.985	1.802	1.850
quintet	0.255	0.066	0.000

[a] Constrained singlet geometry optimization. [b] Constrained triplet geometry optimization. [c] Constrained quintet geometry optimization.

These calculated results are in excellent agreement with what has been observed experimentally in three areas. First, the geometry optimizations show the open-shell quintet to have the lowest overall energy suggesting that the ligand is low field. This agrees well with what has been reported for Fe^{3+}–DAPSC in aqueous solution.[6] Second, the bond distances and associated angles determined in the geometry optimization between the atoms within the immediate coordination sphere of the $[Fe(DAPSC)(H_2O)_2]^{2+}$ species are quite close to that which has been observed in the solid state for the $[Fe(DAPSC)(H_2O)(Cl)]^+$ complex.[4] Finally, the fact that the geometry optimization shows the ligand DAPSC to be planar is indeed significant.

The comparison of the bond distances in Table I clearly shows the reliability of the ZINDO method. Two observations are made as electron density is placed into the $d_{x^2-y^2}$ and d_{z^2} orbitals as the spin multiplicity is changed. First, the bonds to the nitrogen donors become longer, most notably Fe–N2. An electron is now in the $d_{x^2-y^2}$ orbital (i.e. triplet and quintet) increasing the repulsion between the donor electrons and this electron resulting in a longer Fe–N bond length. A similar effect is reflected in the axial bond lengths especially as an electron is placed into the d_{z^2} orbital in the quintet state, which is aligned directly toward the water donors. Second, in going from a singlet to a triplet state, an electron is removed from the d_{xy} orbital and placed into the $d_{x^2-y^2}$ orbital. A notable decrease in the Fe–O1 and Fe–O2 bond length is observed, which is due to the removal of an electron from the d_{xy} orbital directed toward both semicarbazone oxygens resulting in less repulsion and hence a decrease in bond length. Both of these results are reasonable, and they match quite well with the behavior which would be expected.

The agreement of the bond lengths within the equatorial plane determined for the quintet spin state with those observed in the solid sate is extremely good. Although the solid-state complex used in the comparison differs in the axial donors, the five equatorial positions are identical. The ZINDO calculations performed on the $[Fe(DAPSC)(H_2O)_2]^{2+}$ complex assume that there are no external effects contributing to the conformation of the observed complex. In other words, the complex is treated as an isolated system. This is not the case for the geometry of the $[Fe(DAPSC)(H_2O)(Cl)]^+$ complex observed in crystalline form,

---

(11) Palenik, G. J.; Koziol, A. E.; Gawron, M.; Palenik, R. C.; Wester, D. W. *Acta Crystallogr.* **1988**, *C44*, 85.

(12) Pople, J. A.; Beveridge, D. L.; Dobosh, P. A. *J. Chem. Phys.* **1967**, *47*, 2026.

(13) Ridley, J.; Zerner, M. C. *Theor. Chim. Acta* **1973**, *32*, 111.

(14) Bacon, A. D.; Zerner, M. C. *Theor. Chim. Acta* **1979**, *53*, 21.

(15) Anderson, W. P.; Edwards, W. D.; Zerner, M. C. *Inorg. Chem.* **1986**, *25*, 2728.

(16) Zerner, M. C.; Loew, G. H.; Kirchner, R. F.; Mueller-Westerhoff, U. T. *J. Am. Chem. Soc.* **1980**, *102*, 589.

(17) Head, J. D.; Zerner, M. C. *Chem. Phys. Lett.* **1985**, *122*, 264.

(18) Edwards, W. D.; Zerner, M. C. *Theor. Chim. Acta* **1987**, *72*, 347.

Table IV. Molecular Orbital Energies and Relative Total Energies for the Lowest Quintet, Triplet, and Singlet States of the Model Compound (Figure 1)[a]

quintet	triplet	singlet	CAHF
	Molecular Orbital Energies (eV)		
		−5.442 (0) z^2	
	−6.068 (0) z^2	−5.497 (0) $x^2 - y^2$	
−6.640 (0) L*	−6.640 (0) L*	−6.667 (0) L*	−8.245 (0) L*
−6.993 (0) L*	−6.939 (0) L*	−7.021 (0) L*	−8.762 (0) L*
−17.225 (1) z^2			−15.701 (1.2) xy
−17.525 (1) xy	−16.273 (1) xy		−15.756 (1.2) $x^2 - y^2$
−17.769 (1) $x^2 - y^2$	−16.354 (1) $x^2 - y^2$		−15.892 (1.2) z^2
−18.613 (1) xz			−16.572 (1.2) xz
			−16.599 (1.2) yz
		−14.259 (2) xy	
−14.422 (2) L	−14.314 (2) L	−14.341 (2) L	−14.422 (2) L
−15.103 (2) L	−15.075 (2) L	−15.103 (2) L	−15.103 (2) L
−15.810 (2) yz	−15.865 (2) yz	−15.783 (2) yz	
	−16.001 (2) xz	−15.919 (2) xz	
	State Energies Relative to the ROHF Quintet (eV)		
E(SCF) 0.00	1.67	2.70	2.97
E(CAHF)[b] 0.02	1.68	2.33	

[a] The geometry for all calculations reported in this table is that of the quintet. The parameters for these calculations are those appropriate for spectroscopy (see text). The numbers in parentheses are the orbital occupations. [b] Spin-projected CAHF.

which is most certainly affected by near neighbors. Nonetheless, two points can certainly be made. The differences in bond lengths between the quintet spin state, determined to be the lowest in energy from geometry calculations, and those observed via experiment are minor. This close agreement suggests that effects such as packing forces in the solid state are not important in determining the structure of these complexes. Second, three different geometries were clearly distinguished in the calculations, which corresponded to the three different spin states. These results show that the spin state may be one of the most important factors affecting the bond lengths, angles, and geometry observed within the immediate coordination sphere of this type of complex.

Table III displays the total relative energies of the various spin states relative to that of the quintet state, which was found to be the lowest in energy. The geometry constraints are given across the table as column headings and the relative energies for the spin states are listed down the left side as row headings. From Table III it is easy to determine the amount of energy required to go from one spin state to another in a particular geometry or from one spin state in a particular geometry to the same spin state in a different geometry.

In general, Hartree–Fock-based methods tend to favor states of highest multiplicity, yielding them as the lowest energy states. To correct for this generally requires a highly correlated treatment. This bias seems to be eliminated in the INDO method due to its reliance on parameters based on atomic spectroscopy.[15,19,20] Nevertheless, one must remain cautious when using Hartree–Fock theory in examining the differences in spin-state energies.

In order to examine this potential problem somewhat further, we used a configuration averaged Hartree–Fock (CAHF) procedure that averages over all possible electronic states derived from six electrons in five orbitals.[18,21] These results are summarized in Table IV. The energies reported in the bottom of this table are all relative to the quintet SCF. The CAHF results are highest as might be expected as some rather highly excited states are included in the average. The projected CAHF results are obtained from the CAHF calculation through a Rumer diagram (or "valence bond") projection,[22] yielding nearly the same energies as the individual SCF–ROHF calculations have. The exception is in the singlet energy, which has been lowered by some 0.3 eV.

Table V. Excited States of the Quintet Manifold (Energies in 1000 cm^{-1}) with Oscillator Strengths Greater than 10^{-4} Shown in Parentheses

ROHF		CAHF	
1 ref[a]	2 ref[b]	2 ref[b]	comments
1.3 (0)	1.4 (0)	0.2^{++}	$yz \rightarrow xz$
4.6 (0)	4.8 (0)	3.5 (0)	$yz \rightarrow z^2$ [e]
4.8 (0)	4.9 (0)	3.9 (0)	$yz \rightarrow x^2 - y^2$
5.2 (0)	4.2 (0)	4.2 (0)	$yz \rightarrow xy$
18.0 (0)		18.5 (0.0001)	L → L* triplet[c]
18.9 (0)		18.6 (0)	L → L* triplet[c]
		19.1 (0)	L → L* triplet[c]
		19.3 (0)	L → L* triplet[c]
26.6 (0.0006)		26.6 (0.0008)	L → L* triplet[c]
26.8 (0.0005)		26.8 (0.0001)	L → L* triplet[c]
29.9 (0.18)	30.6 (0.227)	30.3 (0.179)	L → L* singlet[d]

[a] The reference is $d_{xy}^2 d_{xz} d_{z^2} d_{x^2-y^2} d_{xy}$. [b] Quintets are generated from both $d_{yz}^2 d_{xz} d_{z^2} d_{x^2-y^2} d_{xy}$ and $d_{yz} d_{xz}^2 d_{z^2} d_{x^2-y^2} d_{xy}$. [c] These are quintet–triplet excitations localized to the ligand (i.e. metal quintet, ligand triplet, overall quintet). [d] These are quintet–singlet excitations localized to the ligand. [e] Excitations involving the d_{z^2} orbital will be quite sensitive to the axial ligand, in this case two water molecules.

This lowering has been effected by a rather large mixing (43%) of the $d_{xz}^2 d_{yz}^2 d_{x^2-y^2}^2$ configuration with the dominant $d_{xz}^2 d_{yz}^2 d_{xy}^2$ one. Of some interest in this calculation is the prediction of the $d_{xz}^2 d_{yz}^2 d_{xy} d_{x^2-y^2}$ singlet state only 40 cm^{-1} higher in energy. This is the singlet component of the lowest energy triplet state that appears in Table IV. For comparison, room-temperature thermal energy is only some 210 cm^{-1} (1 cal/mol = 350 cm^{-1}).

The molecular orbital energies and the relative state energies reported in Table IV are obtained at the quintet geometry reported in Tables I and II. Furthermore, these values are obtained using the spectroscopic INDO/S method known to give good relative energies at fixed geometries using a configuration interaction over single excited states (CIS).[15,16] These values might be compared with those in column 3 of Table III (for the quintet geometry) that were obtained from the geometry optimization and different parameters, showing the consistency of the two methods.

In Table V we report the predicted electronic spectrum of the model compound assuming the quintet ground state and calculated geometry. These calculations contain almost 600 singly excited configurations (CIS), consistent in the manner in which the method was parametrized. Three calculations are shown. The reason for this is that the $d_{yz} \rightarrow d_{xz}$ transition is calculated very low, at 200 cm^{-1}, in the CAHF calculation, prompting a CIS calculation assuming both $d_{yz}^2 d_{xz} d_{z^2} d_{x^2-y^2} d_{xy}$ and $d_{yz} d_{xz}^2 d_{z^2} d_{x^2-y^2} d_{xy}$ reference configurations. The "1 ref" and "2 ref" calculated results do not differ greatly, and all calculations do not differ in their predictions by more than about 1000 cm^{-1}.

It is tempting from these calculations to extract an energy ordering of molecular orbitals. Here some caution must be exercised as orbital energies are not observables but rather only state energies are. These state energies might refer either to excited states or to states obtained through ionization. For d orbitals relaxation is known to be sizeable, shedding considerable doubt on equating the negative of orbital energies with ionization processes (Koopmans' approximation). In addition, in true SCF methods, open-shell orbitals, closed-shell orbitals, and virtual orbitals do not, in general, realize the same Fock potential. This in turn implies that only one set of these orbitals will, in general, obey Koopmans' approximation, not all three. In these cases only open-shell orbitals obey Koopmans' approximation. The combination of this observation, and the fact that relaxation energy itself is very large, leads to, for example, the fact that the singly occupied orbitals of the quintet structure (Table IV) all lie lower in orbital energy than the doubly occupied d_{yz} orbital. Table V, however, verifies the fact that promotion of electrons from the higher lying doubly occupied orbitals (i.e. $d_{yz} \rightarrow d_{z^2}$) leads to a state 3500 cm^{-1} higher in energy.[23]

---

(19) Edwards, W. D.; Weiner, M. C.; Zerner, M. C. *J. Phys. Chem.* **1988**, *92*, 6188.

(20) Axe, F. U.; Flowers, C.; Loew, G. H.; Waleh, A. *J. Am. Chem. Soc.* **1989**, *111*, 7333.

(21) Zerner, M. C. *Int. J. Quant. Chem.* **1989**, *35*, 567.

(22) Pauncz, R. *Spin Eigenfunctions*; Plenum Press: New York, 1979.

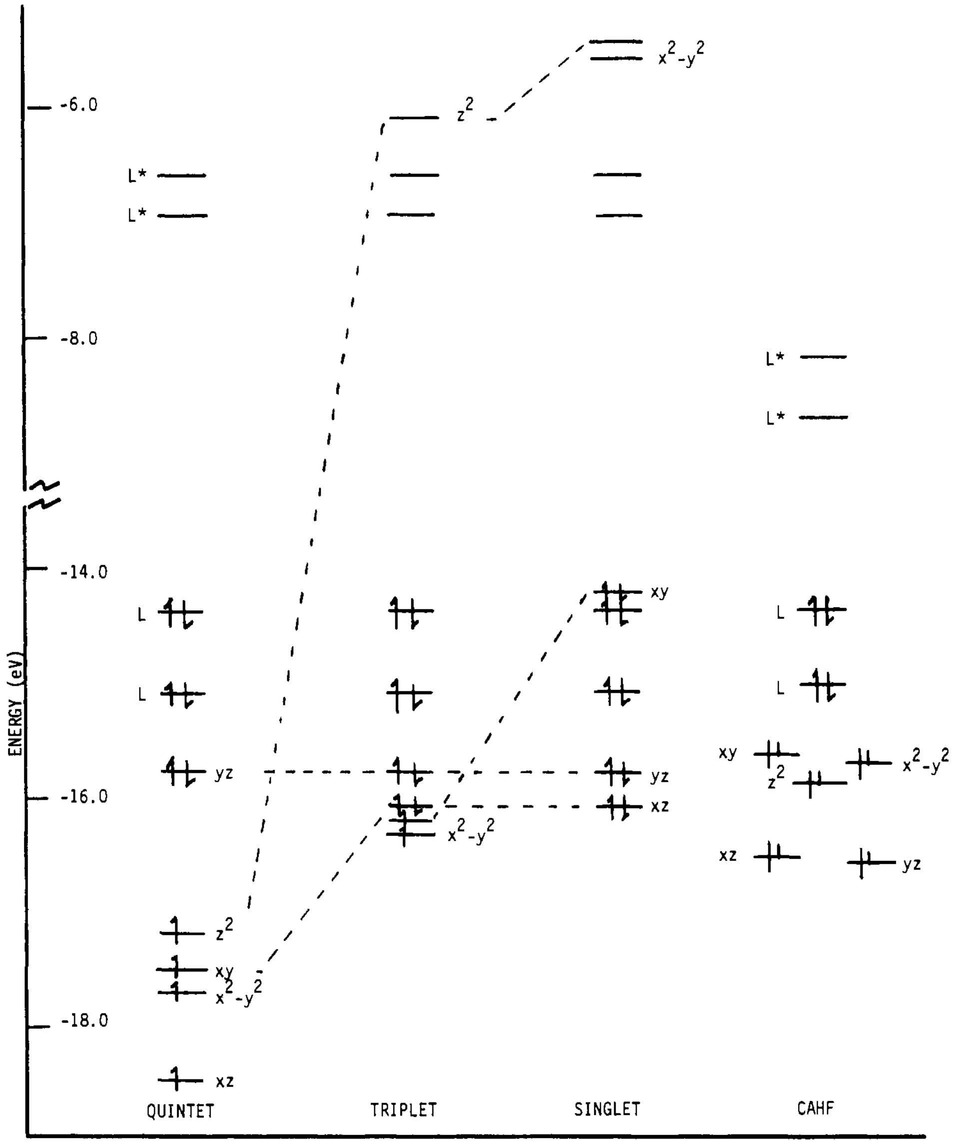

Figure 4. Molecular orbital diagram of $[Fe(DAPSC)(H_2O)_2]^{2+}$ (Figure 1) for different spin states. Note the failure of the Hartree–Fock procedure to obey the aufbau principal for the open-shell systems; see text. In the case of the configuration-averaged Hartree–Fock (CAHF) calculation, the open-shell orbitals all have occupation 1.2.

The orbitals reported in Table IV are shown graphically in Figure 4 to demonstrate further the observations above. In all cases singly or partially filled "d" orbitals lie lower in orbital energy than double-occupied ligand orbitals. L → d excitations give rise to charge-transfer states of considerably higher energy than those whose configurations are presented in the figure. One way to rationalize this is to realize that the gain in coulomb repulsion energy involved in adding an electron to a local d orbital is far greater than that lost by removing it from a very delocalized ligand orbital, and the gain in orbital energy does not compensate for this. Note also that the L* orbital energies of the CAHF calculations appear lower that those obtained from the other calculations, due to the nature of the open-shell operator in this case. Nevertheless L → L* excitations are predicted to lie at nearly the same energy regardless of the L* orbital energies (see Table V for example).

Orbital energies are only useful insofar as they organize our thinking on physical observables. Examining the spectroscopy of Table V suggests $[\epsilon(d_{yz}) \leq \epsilon(d_{xz})] < [\epsilon(d_{z^2})] < [\epsilon(d_{x^2-y^2}) \leq \epsilon(d_{xy})]$. Of considerable interest is the observation that this is the same order as that obtained in Table IV for the CAHF calculation in which all orbitals have the same orbital occupation of 1.2 electrons, and thus all see the same Fock potential. This is not the order given in ref 1, which suggests the general ordering of $[\epsilon(d_{yz}) \approx \epsilon(d_{xz})] < [\epsilon(d_{x^2-y^2}) \approx \epsilon(d_{xy})] < [\epsilon(d_{z^2})]$, but here we must recall that our sixth and seventh axial ligands are water molecules, which are weak ligands and the one that determines the relative ordering of the d_{z^2} orbital.

Conclusions

In this paper the appropriateness of $[Fe(DAPSC)(H_2O)_2]^{2+}$ as a model compound for the theoretical investigation of first-row transition-metal pentagonal-bipyramidal complexes is established. The calculations are able to reproduce the structural parameters associated with the coordination sphere of similar compounds as determined by crystal structures. The ability to reproduce the planarity of the DAPSC ligand around the metal with calculation on an isolated molecule is evidence that the PBP structure is a minimum and not a product of crystal forces in the solid state.

---

(23) In addition to the considerations that limit the utility of Koopmans' approximation mentioned in the text, relaxation, and the fact that open- and closed-shell orbitals both cannot yield orbital energies equal to the negative of ionization potentials, there is also the observation that Koopmans' approximation can only yield ionization potentials between average configurations. For example, if there were no relaxation, the orbital energy of the d_{xz} orbital in the quintet case of Figure 2 would yield an approximation of the ionization potential from quintet state to quartet ion. The loss of an electron from the d_{yz} orbital, however, would yield an approximation of the ionization potential from the quintet state to the average of the resulting sextet and four quartet states but only *after* the appropriate correction to the d_{yz} orbital energy to adjust for the closed-shell Fock potential; see ref 18.

Inorg. Chem. **1992**, *31*, 567-576

With theory more easily than experiment, the structural implications of differing multiplicities of the metal atom can be demonstrated. By the changing of the metal d-orbital populations the bond distances in the coordination sphere adjust as would be expected from simple electrostatic arguments.

Although different in derivation, the spectroscopic theory and the theory developed for geometry demonstrate an underlying consistency as demonstrated here, for example, in very similar predictions of spin-state energies. The pattern of orbital energies has been examined in some detail here, and the dependence of the location of the d$_{z^2}$ orbital energy on the strength of the axial ligands relative to the other ligands is discussed. The generally "assumed" splitting of PBP complexes is two sets of degenerate orbitals lower in energy than the axial orbital. The calculations suggest that this ordering can be changed if the axial ligands are weak field, as here, dropping the axial orbital between the two sets of degenerate orbitals.

In summary, $[Fe(DAPSC)(H_2O)_2]^{2+}$ is ideal as a starting point for the further theoretical and experimental study of PBP complexes, and this is actively being pursued.

Acknowledgment. This work was supported in part through a grant from the Office of Naval Research. J.D.B. is grateful for an Eastman Kodak predoctoral fellowship.

Contribution from the Institut für Technische Elektrochemie,
Technische Universität Wien, Getreidemarkt 9/158, A-1060 Vienna, Austria

Chemical Bonding in Rutile-Type Compounds

Peter I. Sorantin and Karlheinz Schwarz*

Received May 22, 1991

We present an ab initio study of the bonding in the rutile (TiO_2) structure, where the five members TiO_2, VO_2, CrO_2, RuO_2, and ZnF_2 are investigated by means of band structure calculations, from which we derive electron densities, densities of states, total energies, and structure factors. We present simple molecular orbital schemes in order to interpret the main features of the calculated densities of states. Our results show that a MX_6 cluster model (with M = Ti, Zn, V, Cr, or Ru and X = O or F) accounts only for part of the bonding mechanism. In the crystalline environment, the anionic ligands reduce their amount of π-bonding in the MX_6 cluster at the expense of an increased σ-bonding with all three nearest metal neighbors in the M_3X units. This reduction of anionic π-bonding character causes an increase in the metal–metal bonding across the shared edges of MX_6 octahedra. The observed lattice geometry can be seen as the optimum balance between a maximal stabilization of the MX_6 and the M_3X units. In addition, we determine for one example, namely TiO_2, the internal coordinate *u* by minimizing the corresponding total energy and obtain a theoretical *u* of 0.3064 in excellent agreement with the experimental value of 0.305, thus demonstrating the high accuracy of our approach. All calculations are carried out using the full-potential *l*inearized *a*ugmented *p*lane *w*ave (LAPW) method where exchange and correlation effects are treated by the local-density approximation.

1. Introduction

Our interest in the rutile structure type (named after the transition metal (IV)oxide, TiO_2) is motivated by the following four facts: (i) the rutile type is the simplest and most common MX_2 structure where metal atoms M are octahedrally coordinated by ligands X; (ii) in spite of the importance of the rutile structure, we have found only very few theoretical papers most of which are old and do not meet the requirements of modern solid-state chemistry; (iii) the properties of this class of compounds vary wildly from insulating to magnetic and metallic behavior, a variation which is a challenge to theorists; (iv) the rutile type is a demanding test case for applying our procedure of calculating electric field gradients at various atomic sites.

A few additional remarks concerning each of these points are appropriate: Despite the frequent occurrence of this structure type, relatively few related theoretical investigations are found in the literature. The rutile structure is adopted by the transition-metal (IV)oxides and (II)fluorides (3d) TiO_2, VO_2, VF_2, CrO_2, MnO_2, MnF_2, FeF_2, CoF_2, NiF_2, ZnF_2, (4d) RuO_2, PdF_2, and (5d) TaO_2, OsO_2, IrO_2, by the main-group (IV)oxides SiO_2, GeO_2, SnO_2, PbO_2, and by MgF_2. Although structural data are readily available for all of these compounds,[1-7] this has not stimulated much theoretical work with the exception of papers by Baur,[1,2] Goodenough,[8] Caruthers et al.,[9,10] Mattheiss,[11] Gupta et al.,[12] Burdett,[13] Schwarz,[14] Xu et al.,[15] and Glassford et al.[16] Perhaps theorists have been discouraged by the ingenuity of Goodenough's review article[8] on metallic oxides written in 1971. He presented energy diagrams for the common (di)oxide structures to explain the (metallic) behavior of their representatives. His instructive confrontation between experimental data and energy diagrams has substantially influenced work in that field and many interpretations including the present one. However, Goodenough's approach in understanding the properties and bonding in the rutile structure differs significantly from ours; while he built a *phenomenological* model (he calls the chapter on the energy diagrams "Phenomenology") derived from experimental results, our approach is completely *ab initio*. Naturally, there should be a close correspondence between his and our results, and if that is the case,

---

(1) Baur, W. H. *Acta Crystallogr.* **1976**, *B32*, 2200.
(2) Baur, W. H.; Khan, A. A. *Acta Crystallogr.* **1971**, *B27*, 2133.
(3) Baur, W. H. *Acta Crystallogr.* **1961**, *14*, 209.
(4) Rogers, D. B.; Shannon, R. D.; Sleight, A. W.; Gillson, J. L. *Inorg. Chem.* **1969**, *8*, 841.
(5) Restori, R.; Schwarzenbach, D.; Schneider, J. R. *Acta Crystallogr.* **1987**, *B43*, 251.
(6) Gonschorek, W. *Z. Kristallogr.* **1982**, *160*, 187.
(7) Gonschorek, W. *Z. Kristallogr.* **1982**, *161*, 1.
(8) Goodenough, J. B. *Prog. Solid State Chem.* **1971**, *5*, 145.
(9) Caruthers, E.; Kleinman, L.; Zhang, H. I. *Phys. Rev.* **1972**, *B7*, 3753.
(10) Caruthers, E.; Kleinman, L. *Phys. Rev.* **1972**, *B7*, 3760.
(11) Mattheiss, L. F. *Phys. Rev.* **1976**, *B13*, 2433.
(12) Gupta, M.; Freeman, A. J.; Ellis, D. E. *Phys. Rev.* **1977**, *B16*, 3338.
(13) Burdett, J. K. *Inorg. Chem.* **1985**, *24*, 2244.
(14) Schwarz, K. *J. Phys.* **1986**, *F16*, L211.
(15) Xu, J. H.; Jarlborg, T.; Freeman, A. J. *Phys. Rev.* **1989**, *B40*, 7939.
(16) Glassford, K. M.; Troullier, N.; Martins, J. L.; Chelikowsky, J. R. *Solid State Commun.* **1990**, *76*, 635.
(17) Westman, S. *Acta Chem. Scand.* **1961**, *15*, 217.
(18) Porta, P.; Marezio, M.; Remeika, J. P.; Dernier, P. D. *Mater. Res. Bull.* **1972**, *7*, 157.
(19) Boman, C. E. *Acta Chem. Scand.* **1970**, *24*, 116.

0020-1669/92/1331-0567$03.00/0